
Article:
Brulefert, K., Córdova, L.A., Brulin, B. et al. (7 more authors) (2016) Pro-osteoclastic In Vitro Effect of Polyethylene-like Nanoparticles: Involvement in the Pathogenesis of Implant Aseptic Loosening. Journal of Biomedical Research Part A, 104 (11). pp. 2649-2657. ISSN 1549-3296

https://doi.org/10.1002/jbm.a.35803

Pro-osteoclastic *In Vitro* Effect of Polyethylene-like Nanoparticles: Involvement in the Pathogenesis of Implant Aseptic Loosening

Kevin Brulefert [a, b, c*], Luis A. Córdova [a, b, d, *, #], Bénédicte Brulin [a, b], Adrien Faucon [c, e], Philipe Hulin [c, f], Steven Nedellec [c, f], François Gouin [a, b, c], Norbert Passuti [a, b, c], Eléna Ishow [c, e], Dominique Heymann [a, b, c, g]

[a] INSERM, UMR 957, Laboratory of Pathophysiology of Bone Resorption and Therapy of Primary Bone Tumours, 1 rue Gaston Veil, Nantes cedex 1, 44035, Nantes, France.
[b] University of Nantes, Nantes Atlantique Universities, Nantes, France.
[c] Nantes University Hospital, Nantes, France, 1 place Alexis Ricordeau 44093 Nantes Cedex 1.
[d] Department of Oral and Maxillofacial Surgery - Faculty of Dentistry, University of Chile – Conicyt, Santiago, Chile.
[e] CEISAM–UMR CNRS 6230, University of Nantes, Nantes, France.
[f] INSERM, UMS 016-UMS CNRS 3556, MicroPICell platform, SFR Santé François Bonamy, Nantes, France.
[g] Department of Oncology and Metabolism, University of Sheffield, The Medical School, England

[*] Both first authors contributed equally to this manuscript

Kevin Brulefert, brulefert@yahoo.fr
Luis A. Córdova, lcordova@stanford.edu
Bénédicte Brulin, benedicte.brulin@univ-nantes.fr
Adrien Faucon, adrien.faucon@univ-nantes.fr
Philipe Hulin, philippe.hulin@univ-nantes.fr
Steven Nedellec, steven.nedellec@nantes.inserm.fr
François Gouin, francois.gouin@chu-nantes.fr
Norbert Passuti, norbert.passuti@chu-nantes.fr
Eléna Ishow, elena.ishow@univ-nantes.fr
Dominique Heymann, dominique.heymann@sheffield.ac.uk

[#] Corresponding author: Dr. Luis A. Córdova; Current address: Department of Orthopaedic Surgery, School of Medicine, Stanford University, 300 Pasteur Dr, Edward Bd R154, Stanford, CA 94305, Phone: +1(650)-725 6634 United States, e-mail: lcordova@stanford.edu

This article has been accepted for publication and undergone full peer review but has not been through the copyediting, typesetting, pagination and proofreading process which may lead to differences between this version and the Version of Record. Please cite this article as an 'Accepted Article', doi: 10.1002/jbm.a.35803

Abstract

Polyethylene micro-sized wear particles released from orthopaedic implants promote inflammation and osteolysis; however, less is known about the bioactivity of polyethylene nano-sized wear particles released from the last generation of polymer-bearing surfaces. We aim to assess the internalization of fluorescent polyethylene-like nanoparticles by both human macrophages and osteoclasts and also, to determine their effects in osteoclastogenesis *in vitro*. Human macrophages and osteoclasts were incubated with several ratios of fluorescent polyethylene-like nanoparticles between 1-72 hours, and 4 hours, 2, 4, 6 and 9 days respectively. The internalization of nanoparticles was quantified by flow cytometry and followed by both confocal and video time-lapse microscopy. Osteoclast differentiation and activity was semi-quantified by Tartrate-Resistant Acid Phosphatase (TRAP) staining, TRAP mRNA relative expression and pit resorption assay respectively. Macrophages, osteoclast precursors and mature osteoclasts internalized nanoparticles in a dose- and time-dependent manner and maintained their resorptive activity. In addition, nanoparticles significantly increased the osteoclastogenesis as shown by up-regulation of the TRAP expressing cell number. We conclude that polyethylene-like nano-sized wear particles promote osteoclast differentiation without alteration of bone resorptive activity of mature osteoclasts and they could be considered as important actors in periprosthetic osteolysis of the last new generation of polymer-bearing surfaces.

KEYWORDS: Aseptic loosening; Polyethylene; Nanoparticles; Macrophages, Osteoclasts.

1. Introduction

Wear particles released from classic polyethylene surfaces of prosthetic joints constitute the main activator of periprosthetic inflammation and osteolysis leading to aseptic loosening of orthopaedic implants [(1)]. It is admitted that the biological interactions underlying this process are based on the internalization of polyethylene micro-sized wear particles by macrophages with their subsequent activation [(2)]. Consequently, local activated macrophages guide to the recruitment of systemic monocyte-macrophage precursors, leading to the development of a chronically inflamed periprosthetic bone niche and promoting the differentiation of their precursors toward bone resorbing osteoclasts [(3)] (Figure #1 in Supplementary data).

In the last 15 years, cross-linked polyethylene, an optimized high-density polyethylene, has been widely used in clinics, improving the clinical behavior of prosthetic joints assessed for up to 10 years [(4)]. Recent reports based on the long-term follow-up of those prosthesis and joint simulators, describe the presence of significant amount of nano-sized wear particles released from cross-linked polyethylene bearing surfaces [(5)–(9)]. Importantly, these nano-sized wear particles have been reported more bioactive than micro-sized ones when they stimulate clinically relevant cell cultures [(7),(8)]. Nevertheless, the internalization of polyethylene nanoparticles by the monocyte-macrophage-osteoclast lineage and their functional effects on the same cells remain poorly understood. The aim of this study was to assess the internalization of fluorescent polyethylene-like nanoparticles (FPN) by monocyte-macrophage-osteoclast lineage and determine their effect in osteoclastogenesis *in vitro*.

2. Material and methods

2.1. Experimental design

To address our aim we firstly, incubated macrophages, pre-osteoclasts and osteoclasts with specific ratios of customized fluorescent polyethylene-like nanoparticles (described below) per cell at specific time points and then, we assessed their internalization by both fluorescence activated cell-sorting (FACS) and high resolution microscopy methods. Secondly, we quantified the effect of fluorescent polymeric nanoparticles on the osteoclast differentiation by quantifying the expression of Tartrate-Resistant Acid Phosphatase (TRAP).

2.2. Polyethylene Nanoparticles

Aqueous suspensions of fluorescent polyethylene-like nanoparticles (FPN) were obtained from the stiff self-assembling of oligoethylene chains (20 carbon atoms) functionalized with orange-red-emitting fluorophores, and characterized according to Faucon, *et al*. (2013) [(10)] (Figure #2 in Supplementary data). Such FPN contain fluorophores similar to those already exploited as fluorescent and magnetofluorescent nanoparticles to perform *in cellulo* imaging [(11)] and *in vitro* magnetic resonance imaging (MRI) [(12)], respectively. In those cases, cell viability assays showed no detectable cytotoxicity, confirming the biocompatibility of the fluorescent material while strong emissive signal could be observed inside the cells after internalization with no trace of excreted fluorescence over the long term. The mean hydrodynamic diameter D_H was measured to be 169 ± 77 nm by dynamic light scattering (DLS). The colloidal suspension of nanoparticles revealed stable in physiological culture media due to the highly charged surface potential found at -50 mV upon zetametry mesurements. The emission spectrum was centered at λ_{max}(em) = 580 nm after exciting at 488 nm, which limits the contribution of autofluorescence. The absence of

endotoxin was confirmed using a quantitative Limulus Amebocyte Lysate (LAL) assay (Lonza, Belgium) with a threshold of positivity of 0.25 EU/mL.

2.3. Isolation of human CD14$^+$ cells

Ethical approval for the use of peripheral blood from healthy donors was obtained from the Nantes University Hospital Ethics Committee. Samples were obtained from the ‘‘Etablissement Français du Sang’’ with informed consent (agreement reference NTS 2000-24,190 Avenant n°10). Peripheral blood mononuclear cells (PBMC) from seven healthy donors (age= 49.14; range 24-63) were isolated by centrifugation over Ficoll gradient (Sigma, Saint Quentin-Fallavier, France). CD14$^+$ cells were magnetically labeled with CD14 microbeads and positively selected by MACS technology (Miltenyi Biotec, Bergisch Gladbach, Germany). Selected CD14$^+$ cells were analyzed by flow cytometry with a purity of ≥ 95% and the detection of 5%-10% of the CD14$^+$ CD16$^+$ non-classical monocytes. Isolated cells were frozen prior to further experiments. All assays were performed with n=3-5 for each condition and representative of at least two independent experiments.

2.4. Macrophage cell culture

1.5 x 10^6 human blood-derived CD14$^+$ monocytes were seeded in 6-well plate and cultured for 3 days in 2 ml of minimum essential medium alpha (MEM-α, Lonza, Belgium) supplemented with 10% foetal bovine serum (FBS, Ozyme, France), 1% of antibiotics and supplemented with 25 ng/mL of human macrophage colony stimulating factor (hM-CSF, R&D systems, Abingdon, UK) (macrophage growth media). Then, adherent CD14$^+$ cells were cultured in macrophage media as naive macrophages and incubated with three different ratios of FPN per cell during 1, 4, 8, 12,

John Wiley & Sons, Inc.

24, 48 and 72 hours. The three ratios of FPN were theoretically calculated from the stock solution concentration (4 x 10^{10} FPN/mL) and diluting in culture media accordingly. They are 2 x 10^3 FPN per cell (baseline equivalent with 2 x 10^9 FPN/mL), 4 X 10^3 FPN per cell (equivalent with 4 x 10^9 FPN/mL) and 8 x10^3 FPN per cell (equivalent with 8 x 10^9 FPN/mL).

2.5. Osteoclast cell culture and TRAP staining

4.5 x 10^3 and 1.5 x 10^6 human blood-derived $CD14^+$ cells were seeded in 96- and 6-well plates respectively as described [13],[14] and then cultured for 72 hours in macrophage growth media. Then, adherent cells were cultured in macrophage growth media supplemented with 100 ng/ml of human Receptor Activator of Nuclear factor Kappa-B Ligand (hRANKL) (osteoclast differentiation media [ODM]) for up to 11 days (endpoint of osteoclastogenesis). During the early period of culture in ODM (day 2), multinucleated cells with up to 3 nuclei were considered as osteoclast precursors and they were subsequently incubated with FPN for either 4 hours (at day 2 of culture), 2 (corresponding to day 4 of culture), 4 (corresponding to day 6 of culture), 6 (corresponding to day 8 of culture) and 9 (corresponding to day 11 of culture) days. Consequently, multinucleated cells containing more than 3 nuclei were considered as mature osteoclasts and were manually counted under a light microscope (Leica DM IRB, Nanterre, France) after TRAP staining (Sigma) at the endpoint of osteoclastogenesis (day 11 in ODM). Otherwise, 50 x 10^3 $CD14^+$ cells were cultured and differentiated into osteoclasts in 8-well plates (Millicell) using similar protocol focusing confocal microscopy and time-lapse video microscopy assessment.

2.6. Resorption pit assay and scanning electron microscopy

Osteoclast capacity for bone resorption was assessed by pit formation assay [15]. For this purpose,

2 x 10^5 $CD14^+$ human blood-derived $CD14^+$ cells were differentiated into osteoclasts on 5 mm diameter dentin slices in 48 well culture plates using the same protocol. At the end of the culture period (day 11), dentin slices were washed, and adherent osteoclasts and mononuclear cells were removed manually. Resorption pits were assessed qualitatively by scanning electron microscopy (TM3000, Hitachi, Krefeld, Germany).

2.7. Flow cytometry

Adherent macrophages were enzymatically detached using Accutase® cell detachment solution (Life Technologies, Saint Aubin, France). The fluorescence emitted by FPN uptaken by macrophages was assessed by flow cytometry (FC500 Beckman Coulter,Inc. Brea, CA, US) and expressed as the fold change of relative - mean fluorescent intensity (MFI); corresponding to the ratio between the MFI from FPN incubated macrophages over the MFI from control macrophages. Macrophage viability was assessed by DAPI staining on the LSR II Analyzer (BD Immunocytometry Systems, San Diego, CA), using Diva software (BD Immunocytometry Systems, San Diego, CA) for data analysis in the University of Nantes FACS Facility.

2.8. Confocal microscopy

Confocal images of fixed macrophages and osteoclasts stimulated with FPN were carried out using confocal microscopy (Nikon A1 RSi, Nikon, France). Excitation of FPN was performed with a 488 nm laser beam, while their emission was detected at 595/25 nm to identify their localization in both macrophage and osteoclast experiments. F-Actin of macrophage cytoskeleton was stained with phalloidin AlexaFluor546 (Life) whose excitation was performed with a 561 nm laser beam and the emission detected at 595/25 nm. Although the FPN and macrophage cytoskeleton emission signals could be fully be distinguished using distinct excitation

wavelengths, we privileged the use of the more red-shifted phalloidin AlexaFluor647 (Life) that was excited with a 633 nm laser beam, and its emission detected at 700/38 nm to warrantee the clear recognition of both independent fluorescent signals. Nuclei were stained with DAPI (Invitrogen) (excitation with a 405 nm laser beam and emission selected at 450/25 nm in macrophage and osteoclast experiments). The analysis of images was performed using the software Fiji (NIH, USA).

2.9. Time-lapse video microscopy

Consecutives images of macrophages and osteoclasts stimulated with FPN were acquired each 20 and 10 minutes respectively for up 72 hours using light background fluorescence be means of a wide-field microscope (Leica DMI 6000B) (40x). Images were acquired and edited using Metamorph software (Molecular Devices®).

2.10. RNA extraction and quantitative real-time polymerase chain reaction

Total RNA was extracted from cultured cells of each group using homogenizer Ika Ultra-Thurax T 25 (Janke and Kunkel) and TRIzol reagent (Invitrogen). Synthesis of the first strand of complementary DNA and the polymerase chain reaction were carried out in triplicate using the same protocol as described above. The listed oligonucleotides were used to amplify TRAP (5'-AAGACTCACTGGGTGGCTTTG-3' and 3'-GGCAGTCATGGGAGTTCAGG-5'), GADPH (5'-TGGGTGTGAACCATGAGAAGTATG-3' and 3'-GGTGCAGGAGGCATTGCT-5) and B2M *(5'*-TTCTGGCCTGGAGGCTATC-3' and 3'- TCAGGAAATTTGACTTTCCATTC-5') were used as housekeeping genes. Analyses were performed using the Vandesompele method [16].

2.11. Statistical analysis

Results are given as mean ± standard deviation (SD). Unpaired t-test was used to analyse the difference between two groups (MFI fold change in macrophage internalization assays and TRAP fold change). Multiple comparisons were assessed by one-way ANOVA followed by Dunnett's test (number of $TRAP^+$ cells in osteoclastogenesis assays) to compare to the control group. In all cases, differences consider a p value < 0.05. All statistical tests were performed with Graphpad Prism Version 6.0e for Mac OS X (GraphPad Software, La Jolla, CA, USA).

3. Results

3.1. Fluorescent polyethylene-like nanoparticles are internalized by macrophages, osteoclast precursors and mature osteoclasts

We first analyzed the ability of cultured human macrophages to internalize nanoparticles by detecting their fluorescent intensity using flow cytometry. After 48 hours of incubation, FPN were internalized by macrophages in a dose dependent manner as shown by an increase of mean fluorescence intensities (MFI). The internalization of nanoparticles was then significantly up modulated by 2.1, 3.2 and 5.7-fold for the ratio 2 x 10^3, 4 x 10^3 and 8 x 10^3 respectively (Figure 1A). Subsequently, to assess the viability of macrophages exposed to 4 x 10^3 FPN per cell, we quantified the number of dead cells by flow cytometry. No significant increase in macrophage death was observed at 24 hours (8.2%) and 48 hours (6.1%) compared to the control group (7.7%) (Figure 1B). Additionally, a kinetic study of CFPN internalization was also carried out, showing that macrophages internalize FPN from the first hour of exposition demonstrated by a time-dependent increase of MFI (1.5, 2.3, 3.3, 5.1 and 8.6-fold after 1, 4, 8, 12 and 24 hours of incubation with 4 x 10^3 FPN respectively) (Figure 1C).

To determine the location of FPN in macrophages and their impacts on cell morphology, we carried confocal microscopy acquisitions of consecutives stacked cell sections after 48 hours of cell incubation with nanoparticles. This microscopic analysis revealed two patterns of cell morphology were distinguished: a) highly adherent cells, which were characterized by an elongated shape with clustered intracellular FPN (Figure 1D), and b) low adherent cells with a rounded shape containing less amount of cytosolic nanoparticles (Figure 1E). Interestingly, in this later group, FPN were detected in both intracellular and extracellular compartments (Figure 1E, upper left). All the internalized FPN were organized in rounded clusters of variable size

limited by a membrane-like edge, which were detected in a lateral or supra-nuclear position (Figure 1D, orthogonal views); others were identified near to the focal points (Figure 1D). To complete these observations, the internalization of FPN by macrophages was followed by time-lapse microscopy on a 72 hours period (Video Time Lapse #1 in Supplementary Data). First internalization images of FPN were observed 20 minutes after the initial contact between cells and nanoparticles. This internalization took place at one pole of the cell followed by an intracellular trafficking and then, expulsion by a contra-lateral pole. Packed FPN were expulsed to the extracellular compartment 6 hours after the first contact with nanoparticles. Interestingly, this process induced the death of various macrophages (Video Time Lapse #1 in Supplementary Data). Our observations clearly demonstrated that human macrophages were able to internalize FPN in a dose- and time-dependent manner, followed by intracellular processing and packing with subsequent exocytosis of clustered bodies of FPN.

On the other hand, the capacity of osteoclast precursors and mature osteoclasts to internalize FPN was then assessed by confocal microscopy after 4 hours and 9 days of incubation. Both osteoclast precursors and mature osteoclasts exposed for 4 hours to FPN exhibited high capacity to internalize nanoparticles (Figure 2A). After 4 hours of incubation, the fluorescence intensity of FPN in osteoclast precursors appeared stronger than in mature osteoclasts (Figure 2A). In addition, after 9 days of incubation, nanoparticles were always detectable inside mature osteoclasts, however the fluorescence of nanoparticles was heterogeneously distributed and more diffuse compared to the fluorescence detected after 4 hours of exposure (Figure 2A). The internalization ability of osteoclast was confirmed by time-lapse microscopy. Indeed, FPN were internalized by mature osteoclasts at 4 hours of incubation and by osteoclasts precursors after 10 minutes (Video Time Lapse #2 in Supplementary Data). The osteoclasts morphology was then

modified after 9 days of incubation with FPN, exhibiting a rounded shape rather than a square one, as observed in the control cells (Figure 2B, upper). It is important to notice that the osteoclasts challenged with FPN maintained their resorptive function as revealed by a qualitative assessment of resorption pits on dentin slice (Figure 2B, bottom).

3.2. Nanoparticles of polyethylene increase osteoclast differentiation and TRAP expression

To assess the effect of the amount of nanoparticles in osteoclastogenesis, osteoclast precursors were incubated with growing ratios of FPN per cell: 4×10^2, 2×10^3, 4×10^3 and 8×10^3. The number of multinucleated $TRAP^+$ stained cells was determined after 9 days of culture (Figures 3B and 3C). Whereas lower ratios of FPN per cell (4×10^2 and 2×10^3) did not modify the number of osteoclasts compared to the control group, higher ratios significantly increased their number compared to the untreated group (286 ± 73 osteoclasts for ratio 4×10^3; 253 ± 74 osteoclasts for ratio 4×10^3 *versus* 178 ± 41 osteoclasts for control; $p<0.01$ and $p<0.05$ respectively) (Figure 2C, left). Similarly, the number of osteoclasts increased in a time-dependent manner after incubation with 4×10^3 FPN per cell for at least 4 days ($p<0.05$) (Figure 2C, right). We then assessed the mRNA relative expression of TRAP by osteoclasts incubated with the same amount of FPN during 2 (d2), 6 (d6) and 9 (d9) days (Figure 2D). We observed that TRAP expression was up-regulated by 0.5 fold for days 2 ($p<0.0001$) and 6 ($p<0.001$) and 1 fold for day 9 ($p<0.001$) in osteoclasts exposed to FPN compared with osteoclasts non exposed to FPN (Ct). Finally, the osteoclasts challenged with FPN maintained their resorptive function as revealed by a qualitative assessment of resorption pits on dentin slice (Figure 2B, bottom).

4. Discussion

The present study aimed to assess the internalization of polyethylene nanoparticles by monocyte-macrophage-osteoclast lineage using FPN. In addition, the impact of FPN on osteoclastogenesis and osteoclast activity in the context of wear-particles induced osteolysis was analyzed. We demonstrated the intracellular uptake of FPN by both macrophages and osteoclasts promotes osteoclast differentiation. Despite to the reported inter-individual variability of the monocyte-derived lineage response under different stimuli [17], our data underline an important role or FPN in the dysregulation of healthy human macrophages and osteoclasts *in vitro*. These findings could be associated with the pathophysiologic events of aseptic loosening of orthopaedic implants.

The study of the effect of polyethylene nano-sized wear particles on monocyte-macrophage-osteoclast lineage response is a relevant topic in orthopaedic research. Indeed, previous studies demonstrated the effects of the size and composition of wear-particles on macrophage bioactivity [18],[19]. Authors found, an inversed correlation between particle size and biological activity according with their volumetric concentration [18]. With this regard, FPN used in our study constitute a relevant model of polyethylene nanoparticles by both their size (169 ± 77 nm) and their polymeric nature. In fact, these nanoparticles are in the size range of those retrieved from human periprosthetic tissues, reported as important promoter of periprosthetic chronic inflammation [5],[6],[9]. Moreover, they polymeric composition by customization with long alkyl chains containing 20 carbon atoms and the high payload of up to 10^5 closely packed molecules per nanoparticle, also gather the composition and density of retrieved polyethylene wear debris [5],[6],[9]. Importantly, polymeric chains were reported acting as danger associated molecular patterns (DAMPs), being recognized by specific toll-like receptors (TLRs) in macrophages [17]. The recognition of DAMPs by TLRs is an crucial step in the classical activation of naïve

macrophages to the pro-inflammatory phenotype [17]. Finally, these nanoparticles are detectable and biocompatible by presenting fluorophores akin to those used in fluorescent and magnetofluorescent nanoparticles exploited for *in cellulo* [11] and *in vitro* MRI imaging [12]. In those cases, cell viability assays showed no detectable cytotoxicity, confirming the biocompatibility of fluorescent organic nanoparticles while strong emissive signal could be observed inside the cells after internalization. Moreover, we established a culture system of macrophages and osteoclasts exposed to nanoparticles in suspension overcoming the technical limitations reported for classical bi-dimensional culture systems challenged with polyethylene particles [20]. Indeed, this model allowed the homogenous exposition of nanoparticles to adherent macrophages/osteoclasts, avoiding the physical separation between particles (floating in the top of culture media) and cells (bottom of the well) [20],[21]. The fluorescence property of nanoparticles enabled efficient detection and straightforward follow-up using routine methods. In addition, MFI value was an original parameter to semi-quantify the fluorescent intensity of nanoparticles uptaken by macrophages. This method is then a cost-effective and reliable way to assess the nanoparticle traffic in monocyte-derived cell cultures.

We next confirmed the intracellular location of FPN in both macrophages and osteoclasts, using confocal and video time-lapse microscopy. After quick internalization by macrophages (20 minutes), FPN were aggregated in small and large clusters and appear to be enveloped by a membrane-like structure. From 1 hour to 48 hours, macrophages randomly exocytosed a less fluorescent and clustered nanoparticles to the extracellular media continuously limited by a membrane-like structure. Following this process, some macrophages modified their morphology, lost their attachment and died. Interestingly, osteoclast precursors and mature osteoclasts also internalized nanoparticles, clustering and dissociating them in their intracellular compartment.

These findings could be related by the common hematopoietic/mononuclear cell origin of both macrophages and osteoclasts. Thus, their capability to internalize cell debris, micro- and nanoparticles are related to a typical feature of phagoctytic cells. Passive endocytosis of nanoparticles of 100-200 nm has been also reported in various cell types, including HeLa cells, mesenchymal stem cells and osteoblasts [(22)–(24)]. While the nanoparticle size used in this study was 169 ± 77 nm, the methods used in our study did not allow to define the exact mechanism underlying their internalization, constituting one of the limitations of the current study.

The intracellular dissociation and subsequent clustering of FPN observed in both macrophages and osteoclasts, strongly suggests that they were trafficked in the intracellular compartments of these cells, presumably by the endolysosomic pathway [(7),(25),(26)]. In fact, once FPN were internalized by macrophages, they were rapidly clustered and limited by membrane-like structures and then mobilized from one pole of the cell (internalization pole) to the opposite (exocytose pole) followed by the release of the clustered fluorescent bodies in the extracellular compartment and cell death. The traffic of nanoparticles in macrophages through endolysosome compartment with subsequent cell damages and death, has been previously observed by Maitra *et al.* (2009) [(7)]. In fact, these authors associated this trafficking with endosomal damage, cell stress and activation of the NALP3 inflammasome [(7)]. Regarding this mechanism, the involvement of Cathepsin B, interleukin (IL) -1 β and IL-18 and the induction of inflammatory programed cell death (pyroptosis) have also been proposed as a mechanism involved in cell death under inflammatory environment [(7),(27),(28)].

Finally, osteoclast precursors enhanced osteoclast differentiation *in vitro* in a dose- and time-dependent manner after exposition to FPN. The growing upregulation of TRAP expression confirm the functional activation induced by internalized FPN on both osteoclast precursors (at day 2-6 of exposition) and mature osteoclasts (at day 9 of exposition). However, the number of mature osteoclasts only increased when osteoclast precursors were exposed to FPN for at least 4 days (Figure 2C). While the osteoclastogenesis is mainly promoted by RANKL-producing osteoblasts, several stimuli, including LPS [29], may also up regulate the exacerbated bone resorption. In our study, we exclusively induced osteoclastogenesis by adding exogenous RANKL to macrophages challenged by LPS-free FPN, in order to exclude a secondary pro-osteoclastogenic stimulus. On other hand, the observed time-dependent osteoclastogenesis may be associated with the reported early activation of both nuclear factor kappa-B (NF-kB) and nuclear factor of activated T-cells (NFAT) pathways in osteoclast precursors incubated with polymethylmethacrylate (PMMA) particles [30],[31]. These observations are in agreement with clinical scenario, where macrophages present in the periprosthetic tissue are exposed to cumulative volumes of nano-sized wear particles continuously released from bearing surfaces [9],[32]. We observed a clear difference in the morphology of osteoclasts exposed to FPN with maintenance of their resorptive activity. These findings would suggest a reorganization of the cytoskeleton attributable to FPN challenge, however the interpretation of them remains limited due the qualitative nature of this assessment. Further functional studies are needed to elucidate the impact of FPN on the reorganization of cytoskeleton and function.

FPN are internalized by macrophages and are able to promote osteoclast differentiation. An assessment of these two key events described in particle-induced inflammation and osteolysis will be necessary in pre-clinical animal models [33]. The first objective of *in vivo* assessment

should be to determine if FPN are able to induce inflammatory and osteolytic changes in a bone site. To address this subject, the use of the cost-effective calvaria mouse model appears very appropriate as a first step. This model allows a quick assessment of both inflammation and osteolysis in an orthotopic site [33]. Our group recently reported inflammatory and osteolytic changes starting at day 7 after surgical micro-particle (6 μm) implantation [3]. On other hand, Goodman's group reported the feasibility to induce osteolysis in the same model by the transcutaneous implantation of micro-particle in a smaller range, reducing the potential bias of inflammation due to the surgical approach [34]. Based on these reports, it may possible to carry out the implantation of these FPN in a bone site by transcutaneous injection. The second step will be an infusion of FPN into the epiphysis of a long bone using the continuous infusion femoral model, the most clinically relevant mouse model in this field [32],[33].

In summary, FPN are internalized by macrophages, osteoclast precursors and also by mature osteoclasts in a time- and dose-dependent manner. FPN exhibit a pro-osteoclastic effect when they were exposed to osteoclast precursors for at least 4 days. Our results strongly suggest that polyethylene nano-sized wear particles have a pro-osteoclastogenic effect and identify them as potential new actors in the pathogenesis of aseptic loosening of the current generation of polyethylene bearing surfaces (Figure 3). Further comparative studies are needed to elucidate the relevance of nano-sized wear particles compared with standardized stimulus in cell models of aseptic loosening.

Acknowledgements

Financial support for this research was provided by the "Agence Nationale de la Recherche" - GRANT 2007 Pathophysiology of Human Diseases Project N°RO 7196N, INSERM, University of Nantes, University of Chile, CONICYT- Becas Chile and by "Société Civile de Brevets et Recherches sur les Implants Osseux Hip-Care".

References

1. Cobelli N, Scharf B, Crisi GM, Hardin J, Santambrogio L. Mediators of the inflammatory response to joint replacement devices. Nat Rev Rheumatol. 2011;7:600–8.
2. Purdue PE, Koulouvaris P, Potter HG, Nestor BJ, Sculco TP. The cellular and molecular biology of periprosthetic osteolysis. Clin Orthop Relat Res. 2007;454:251–61.
3. Cordova LA, Trichet V, Escriou V, Rosset P, Amiaud J, Battaglia S, Charrier C, Berreur M, Brion R, Gouin F, Layrolle P, Passuti N, Heymann D. Inhibition of osteolysis and increase of bone formation after local administration of siRNA-targeting RANK in a polyethylene particle-induced osteolysis model. Acta Biomater. 2015;13:150–8.
4. Glyn-Jones S, Thomas GE, Garfjeld-Roberts P, Gundle R, Taylor A, McLardy-Smith P, Murray DW. The John Charnley Award: Highly crosslinked polyethylene in total hip arthroplasty decreases long-term wear: a double-blind randomized trial. Clin Orthop Relat Res. 2015;473:432–8.
5. Galvin AL, Tipper JL, Ingham E, Fisher J. Nanometre size wear debris generated from crosslinked and non-crosslinked ultra high molecular weight polyethylene in artificial joints. Wear. 2005;259:977–83.
6. Ma N, Ma C, Li C, Wang T, Tang Y, Wang H, Moul X, Chen Z, Hel N. Influence of nanoparticle shape, size, and surface functionalization on cellular uptake. J Nanosci Nanotechnol. 2013;13:6485–98.
7. Maitra R, Clement CC, Scharf B, Crisi GM, Chitta S, Paget D, Purdue PE, Cobelli N, Santambrogio L. Endosomal damage and TLR2 mediated inflammasome activation by alkane particles in the generation of aseptic osteolysis. Mol Immunol. 2009;47:175–84.
8. Pal N, Quah B, Smith PN, Gladkis LL, Timmers H, Li RW. Nano-osteoimmunology as an important consideration in the design of future implants. Acta Biomater. 2011;7:2926–34.
9. Richards L, Brown C, Stone MH, Fisher J, Ingham E, Tipper JL. Identification of nanometre-sized ultra-high molecular weight polyethylene wear particles in samples retrieved in vivo. J Bone Joint Surg Br. 2008;90:1106–13.
10. Faucon A, Lenk R, Hémez J, Gautron E, Jacquemin D, Questel J-YL, Graton J, Brosseau A, Ishow E. Fluorescent carboxylic and phosphonic acids: comparative photophysics from solution to organic nanoparticles. Phys Chem Chem Phys. 2013;15:12748–56.
11. Breton M PG Audibert JF, et al. Solvatochromic dissociation of non-covalent fluorescent organic nanoparticles upon cell internalization. Chem Mater. 2011;3:13268–76.
12. Faucon A, Maldiney T, Clément O, Hulin P, Nedellec S, Robard M, Gautier N, Meulenaere ED, Clays K, Orlando T, Lascialfari A, Fiorini-Debuisschert C, Fresnais J, Ishow E. Highly cohesive dual nanoassemblies for complementary multiscale bioimaging. J Mater Chem B. 2014;2:7747–55.
13. Duplomb L, Baud'huin M, Charrier C, Berreur M, Trichet V, Blanchard F, Heymann D. Interleukin-6 inhibits receptor activator of nuclear factor kappaB ligand-induced osteoclastogenesis by diverting cells into the macrophage lineage: key role of Serine727 phosphorylation of signal transducer and activator of transcription 3. Endocrinology. 2008;149:3688–97.
14. Baud'huin M, Renault R, Charrier C, Riet A, Moreau A, Brion R, Gouin F,

Duplomb L, Heymann D. Interleukin-34 is expressed by giant cell tumours of bone and plays a key role in RANKL-induced osteoclastogenesis. J Pathol. 2010;221:77–86.
15. Teletchea S, Stresing V, Hervouet S, Baud'huin M, Heymann MF, Bertho G, Charrier C, Ando K, Heymann D. Novel RANK antagonists for the treatment of bone-resorptive disease: theoretical predictions and experimental validation. J Bone Min Res. 2014;29:1466–77.
16. Vandesompele J, De Preter K, Pattyn F, Poppe B, Van Roy N, De Paepe A, Speleman F. Accurate normalization of real-time quantitative RT-PCR data by geometric averaging of multiple internal control genes. Genome Biol. 2002;3:RESEARCH0034.
17. Ma J, Chen T, Mandelin J, Ceponis A, Miller NE, Hukkanen M, Ma GF, Konttinen YT. Regulation of macrophage activation. Cell Mol Life Sci CMLS. 2003;60:2334–46.
18. Green TR, Fisher J, Matthews JB, Stone MH, Ingham E. Effect of size and dose on bone resorption activity of macrophages by in vitro clinically relevant ultra high molecular weight polyethylene particles. J Biomed Mater Res. 2000;53:490–7.
19. Matthews JB, Besong AA, Green TR, Stone MH, Wroblewski BM, Fisher J, Ingham E. Evaluation of the response of primary human peripheral blood mononuclear phagocytes to challenge with in vitro generated clinically relevant UHMWPE particles of known size and dose. J Biomed Mater Res. 2000;52:296–307.
20. Fang H-W, Ho Y-C, Yang C-B, Liu H-L, Ho F-Y, Lu Y-C, Ma H-M, Huang C-H. Preparation of UHMWPE particles and establishment of inverted macrophage cell model to investigate wear particles induced bioactivites. J Biochem Biophys Methods. 2006;68:175–87.
21. Ingram JH, Stone M, Fisher J, Ingham E. The influence of molecular weight, crosslinking and counterface roughness on TNF-alpha production by macrophages in response to ultra high molecular weight polyethylene particles. Biomaterials. 2004;25:3511–22.
22. Dausend J, Musyanovych A, Dass M, Walther P, Schrezenmeier H, Landfester K, Mailänder V. Uptake mechanism of oppositely charged fluorescent nanoparticles in HeLa cells. Macromol Biosci. 2008;8:1135–43.
23. Gratton SEA, Ropp PA, Pohlhaus PD, Luft JC, Madden VJ, Napier ME, DeSimone JM. The effect of particle design on cellular internalization pathways. Proc Natl Acad Sci. 2008;105:11613–8.
24. Holzapfel V, Musyanovych A, Landfester K, Lorenz MR, Mailänder V. Preparation of Fluorescent Carboxyl and Amino Functionalized Polystyrene Particles by Miniemulsion Polymerization as Markers for Cells. Macromol Chem Phys. 2005;206:2440–9.
25. Heymann D, Pradal G, Benahmed M. Cellular mechanisms of calcium phosphate ceramic degradation. Histol Histopathol. 1999;14:871–7.
26. Benahmed MD, Heymann D, Berreur M, Cottrel M, Godard A, Daculsi G, Pradal G. Ultrastructural study of degradation of calcium phosphate ceramic by human monocytes and modulation of this activity by HILDA/LIF cytokine. J Histochem Cytochem. 1996;44:1131–40.
27. Hornung V, Bauernfeind F, Halle A, Samstad EO, Kono H, Rock KL, Fitzgerald KA, Latz E. Silica crystals and aluminum salts activate the NALP3 inflammasome through phagosomal destabilization. Nat Immunol. 2008;9:847–56.
28. Scharf B, Clement CC, Wu XX, Morozova K, Zanolini D, Follenzi A, Larocca JN, Levon K, Sutterwala FS, Rand J, Cobelli N, Purdue E, Hajjar KA, Santambrogio L.

Annexin A2 binds to endosomes following organelle destabilization by particulate wear debris. Nat Commun. 2012;3:755.
29. Yoshimatsu M, Kitaura H, Fujimura Y, Kohara H, Morita Y, Yoshida N, Yoshimatsu M, Kitaura H, Fujimura Y, Kohara H, Morita Y, Yoshida N. IL-12 Inhibits Lipopolysaccharide Stimulated Osteoclastogenesis in Mice, IL-12 Inhibits Lipopolysaccharide Stimulated Osteoclastogenesis in Mice. J Immunol Res J Immunol Res. 2015;2015, 2015:e214878.
30. Yamanaka Y, Abu-Amer W, Foglia D, Otero J, Clohisy JC, Abu-Amer Y. NFAT2 Is an essential mediator of orthopedic particle-induced osteoclastogenesis. J Orthop Res. 2008;26:1577–84.
31. Yamanaka Y, Karuppaiah K, Abu-Amer Y. Polyubiquitination events mediate polymethylmethacrylate (PMMA) particle activation of NF-kappaB pathway. J Biol Chem. 2011;286:23735–41.
32. Ren P-G, Irani A, Huang Z, Ma T, Biswal S, Goodman SB. Continuous infusion of UHMWPE particles induces increased bone macrophages and osteolysis. Clin Orthop. 2011;469:113–22.
33. Cordova LA, Stresing V, Gobin B, Rosset P, Passuti N, Gouin F, Trichet V, Layrolle P, Heymann D. Orthopaedic implant failure: aseptic implant loosening-the contribution and future challenges of mouse models in translational research. Clin Sci Lond Engl 1979. 2014;127:277–93.
34. Rao AJ, Zwingenberger S, Valladares R, Li C, Smith RL, Goodman SB, Nich C. Direct subcutaneous injection of polyethylene particles over the murine calvaria results in dramatic osteolysis. Int Orthop. 2013;37:1393–8.

Figure Legends

Figure 1. Human macrophages internalize FPN in a dose- and time-dependent manner. A) Macrophages were incubated with three ratios of FPN per cell for 48 hours. B) Macrophage viability (DAPI staining) after FPN exposure for up to 48 hours. C) Kinetic assessment of the FPN uptake by macrophages. D) Highly adherent macrophages exhibited clustered FPN in the intracellular compartment. E) Clustered FPN were mostly detected in the extracellular media rather than in the cytosolic compartment of low adherent macrophages. Both D and E images were acquired by confocal microscopy from macrophage cell cultures exposed during 48 hours to FPN (*green, FPN; red, actin cytoskeleton and blue, DAPI stained nuclei).*

Fluorescent polyethylene-like nanoparticles (FPN), Mean Fluorescent intensity (MFI), $p < 0.05$ (*), $p < 0.01$ (**) and $p < 0.001$ (***).

Figure 2. FPN are internalized by human osteoclast precursors and mature osteoclasts increasing osteoclastogenesis and TRAP expression. A) FPN were detected in the intracellular compartment of both osteoclast precursors at 4 hrs (orthogonal sections, left picture) and osteoclasts after 4 hours and 9 days of incubation (orthogonal sections, right pictures) using confocal microscopy (*green, FPN; violet, actin cytoskeleton and blue, DAPI stained nuclei)*. B) Osteoclasts were identified by TRAP staining and their activity was detected by scanning electron microscopy of the pit resorption assay on dentin slice. C) The number of $TRAP^+$ multinucleated cells (osteoclasts) was quantified at endpoint according to several doses (left panel) and time of exposition to FPN (right panel). D) The relative expression of TRAP by osteoclasts exposed to FPN at three time points was expressed as fold-change. Fluorescent polyethylene-like nanoparticles (FPN), Osteoclast precursors (OCP), Mature osteoclasts (OCs), Fold-change (Fc), $p < 0.05$ (*), $p < 0.01$ (**), $p < 0.001$ (***), $p < 0.0001$ (****).

Figure 3. Modelization of the pro-osteoclastic effect exerted by polyethylene nano-sized wear particles

Supplementary data

Figure #1. Peri-acetabular osteolysis by polyethylene wear debris. A) AP pelvis x-ray of revised right metal-polyethylene THA in a 73-year-old-woman secondary to congenital hip dysplasia. B) and C) Zoomed views of 2013 (B) and 2014 (C) AP pelvis x-rays showing the incremental radiolucency (osteolysis) around the acetabular component (black arrows) of THA in the same patient. Osteolysis is the consequence of cumulative rates of wear debris particles released from frictional bearing surfaces of the THA. D) Polarized histological view of the periprosthetic interface in an experimental model of polyethylene-particle osteolysis (Córdova LA, 2014). Chronic inflammatory response (*) induced by polyethylene wear particles (white arrows), which are in close relationship with osteoclast-like cells (translucid arrows) identified on their bone resorptive lacunae.

Antero-posterior (AP), Total Hip Replacement (THA)

Figure #2 . Chemical and physical characterization of FPN

A) Chemical structure: (E)-icosyl 3-(4-(bis(4'-(tert-butyl)-[1,1'-biphenyl]-4-yl)amino)phenyl)-2-cyanoacrylate. B) Water-suspended FPN by TEM C) Diameter and dispersivity of FPN by DLS Fluorescent polyethylene-like nanoparticles (FPN); Transmission electron microscopy (TEM); Dynamic light scattering (DLS).

Video time lapse #1. Internalization, intracellular trafficking and exocytosis of FPN by macrophages. Macrophages were incubated with FPN at ratio of 4 x 10^3 nanoparticles per cell and then followed by video time-lapse microscopy including one acquisition every 20 minutes during 48 hours. Once FPN were internalized, they were trafficked intracellularily and then exocytosed to the extracellular media. Some cells dead after exocytosis. Fluorescent polyethylene-like nanoparticles (FPN)

Video time lapse #2. Internalization of FPN by both mature osteoclasts and osteoclasts precursors. Osteoclasts (Ocs) and their precursors (OCP) were incubated with FPN at ratio of 4 x 10^3 nanoparticles per cell and then followed by video time-lapse microscopy including one acquisition every 10 minutes during 48 hours. Osteoclasts internalize FPN identified by localized red fluorescence (white arrow). Otherwise, osteoclast precursors actively internalize FPN, keeping them diffusely in the intracellular compartment. Fluorescent polyethylene-like nanoparticles (FPN), Osteoclast precursors (OCP), Mature osteoclasts (OCs).

Figure 1

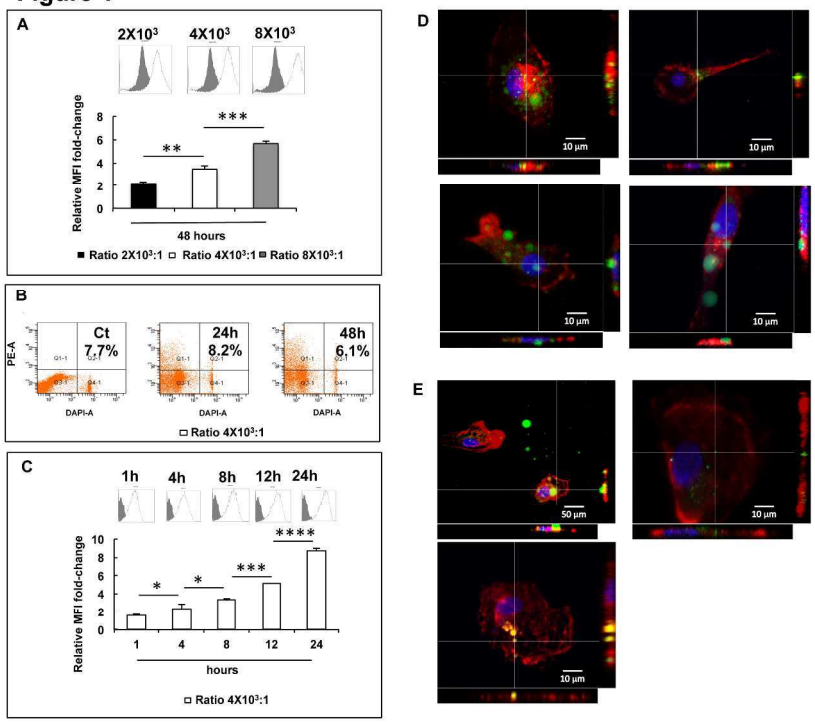

Figure 1. Human macrophages internalize FPN in a dose- and time-dependent manner. A) Macrophages were incubated with three ratios of FPN per cell for 48 hours. B) Macrophage viability (DAPI staining) after FPN exposure for up to 48 hours. C) Kinetic assessment of the FPN uptake by macrophages. D) Highly adherent macrophages exhibited clustered FPN in the intracellular compartment. E) Clustered FPN were mostly detected in the extracellular media rather than in the cytosolic compartment of low adherent macrophages. Both D and E images were acquired by confocal microscopy from macrophage cell cultures exposed during 48 hours to FPN (green, FPN; red, actin cytoskeleton and blue, DAPI stained nuclei). Fluorescent polyethylene-like nanoparticles (FPN), Mean Fluorescent intensity (MFI), $p < 0.05$ (*), $p < 0.01$ (**) and $p < 0.001$ (***).
254x190mm (300 x 300 DPI)

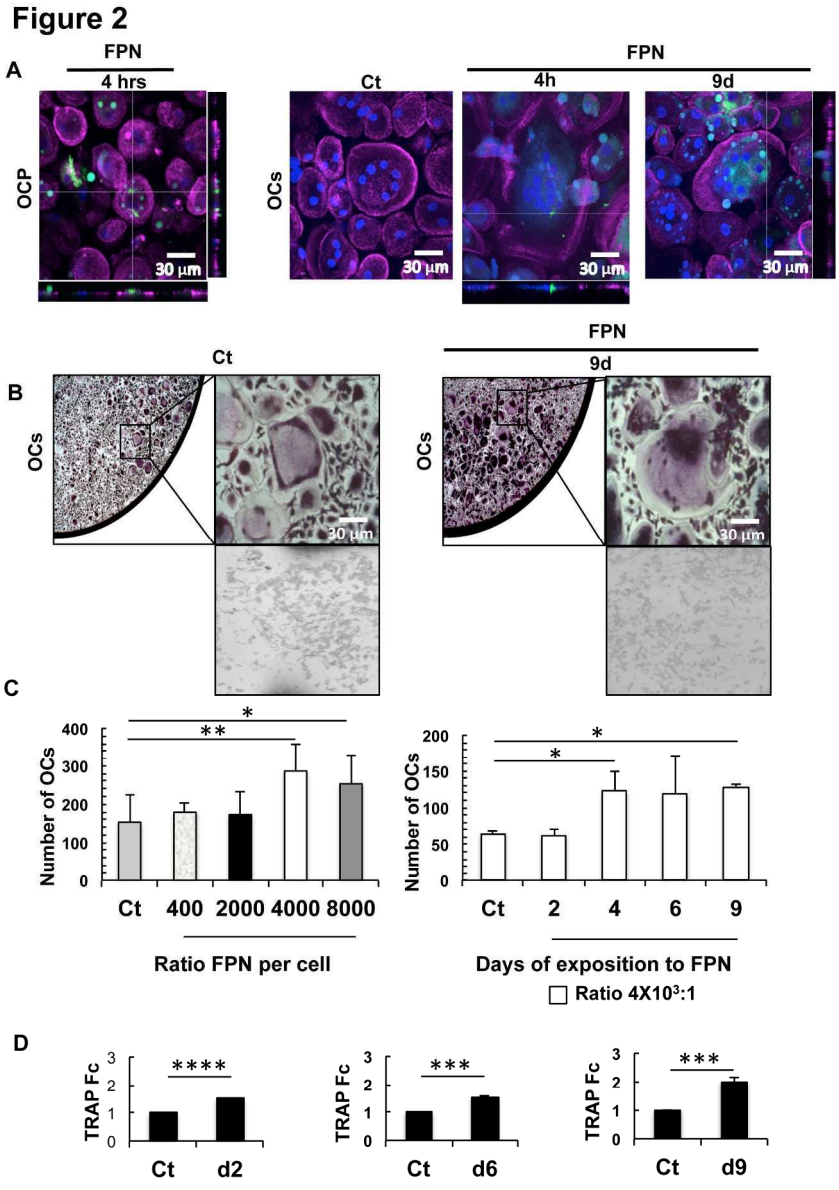

Figure 2. FPN are internalized by human osteoclast precursors and mature osteoclasts increasing osteoclastogenesis and TRAP expression. A) FPN were detected in the intracellular compartment of both osteoclast precursors at 4 hrs (orthogonal sections, left picture) and osteoclasts after 4 hours and 9 days of incubation (orthogonal sections, right pictures) using confocal microscopy (green, FPN; violet, actin cytoskeleton and blue, DAPI stained nuclei). B) Osteoclasts were identified by TRAP staining and their activity was detected by scanning electron microscopy of the pit resorption assay on dentin slice. C) The number of TRAP+ multinucleated cells (osteoclasts) was quantified at endpoint according to several doses (left panel) and time of exposition to FPN (right panel). D) The relative expression of TRAP by osteoclasts exposed to FPN at three time points was expressed as fold-change. Fluorescent polyethylene-like nanoparticles (FPN), Osteoclast precursors (OCP), Mature osteoclasts (OCs), Fold-change (Fc), $p < 0.05$ (*), $p < 0.01$ (**), $p < 0.001$ (***), $p < 0.0001$ (****).
190x254mm (300 x 300 DPI)

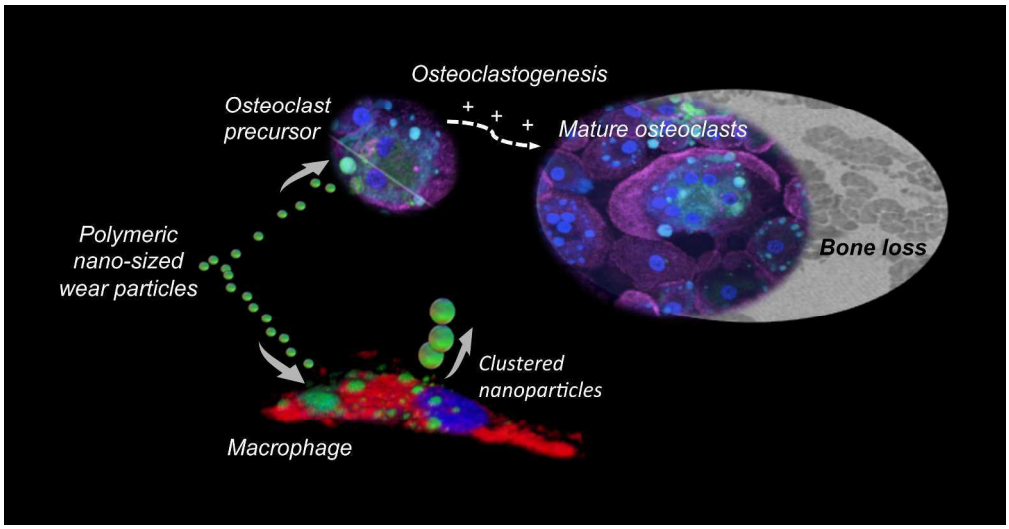

Figure 3. Modelization of the pro-osteoclastic effect exerted by polyethylene nano-sized wear particles
240x124mm (300 x 300 DPI)